Biometals (2024) 37:115–130
https://doi.org/10.1007/s10534-023-00532-7

RESEARCH

Antibacterial and antioxidant activity of gold and silver nanoparticles in dextran–polyacrylamide copolymers

Anton Tkachenko · Sadin Özdemir · Gülşah Tollu · Nadir Dizge · Kasim Ocakoglu · Volodymyr Prokopiuk · Anatolii Onishchenko · Vasyl Chumachenko · Pavlo Virych · Vadym Pavlenko · Nataliya Kutsevol

Received: 4 April 2023 / Accepted: 22 August 2023 / Published online: 31 August 2023

Abstract Search for new antimicrobial agents is of great significance due to the issue of antimicrobial resistance, which nowadays has become more important than many diseases. The aim of this study was to evaluate the toxicity and biological effects of a dextran-graft-polyacrylamide (D-PAA) polymer-nanocarrier with/without silver or gold nanoparticles (AgNPs/D-PAA and AuNPs/D-PAA, respectively) to analyze their potential to replace or supplement conventional antibiotic therapy. The toxicity of nanocomplexes against eukaryotic cells was assessed on primary dermal fibroblasts using scratch, micronucleus and proliferation assays. DPPH (2,2-diphenyl-1-picrylhydrazylradical) assay was used to evaluate the antioxidant capacity of D-PAA, AgNPs/D-PAA and AuNPs/D-PAA. DNA cleavage, antimicrobial and biofilm inhibition effects of nanocomplexes were investigated. Nanocomplexes were found to be of moderate toxicity against fibroblasts with no genotoxicity observed. AgNPs/D-PAA reduced motility and proliferation at lower concentrations compared with the other studied nanomaterials. AgNPs/D-PAA and AuNPs/D-PAA showed radical scavenging capacities in a dose-dependent manner. The antimicrobial activity of AgNPs/D-PAA against various bacteria was found to be much higher compared to D-PAA and AuNPs/D-PAA, especially against *E. hirae, E. faecalis* and *S. aureus*, respectively. D-PAA, AgNPs/D-PAA and AuNPs/D-PAA showed DNA-cleaving and biofilm inhibitory activity, while AgNPs/D-PAA displayed the highest anti-biofilm activity. AgNPs/D-PAA and AuNPs/D-PAA were characterized by good

A. Tkachenko (✉) · V. Prokopiuk · A. Onishchenko
Research Institute of Experimental and Clinical Medicine, Kharkiv National Medical University, Kharkiv 61022, Ukraine
e-mail: as.tkachenko@knmu.edu.ua

S. Özdemir
Food Processing Programme, Technical Science Vocational School, Mersin University, 33343 Yenişehir, Mersin, Turkey

G. Tollu
Laboratory and Veterinary Health, Technical Science Vocational School, Mersin University, 33343 Yenişehir, Mersin, Turkey

N. Dizge (✉)
Department of Environmental Engineering, Mersin University, 33343 Yenişehir, Mersin, Turkey
e-mail: nadirdizge@gmail.com

K. Ocakoglu
Department of Eng. Fundamental Sciences, Faculty of Engineering, Tarsus University, 33400 Tarsus, Turkey

V. Prokopiuk
Department of Cryobiochemistry, Institute for Problems of Cryobiology and Cryomedicine, National Academy of Sciences of Ukraine, Kharkiv 61015, Ukraine

V. Chumachenko · P. Virych · V. Pavlenko · N. Kutsevol
Faculty of Chemistry, Taras Shevchenko University of Kyiv, Kyiv 01601, Ukraine

antimicrobial activity. According to the findings of the study, AgNPs/D-PAA and AuNPs/D-PAA can be evaluated as alternatives for the preparation of new antimicrobial agents, the fight against biofilms, sterilization and disinfection processes. Our findings confirm the versatility of nanosystems based on dextran–polyacrylamide polymers and indicate that AgNPs/D-PAA and AuNPs/D-PAA can be evaluated as alternatives for the preparation of novel antimicrobial agents.

Keywords Gold nanoparticles · Silver nanoparticles · Antimicrobial activity · Antioxidant · DNA cleavage

Introduction

Gold (Au) and silver (Ag) nanoparticles (NPs) are currently under vigorous investigation as potential antimicrobial agents that can contribute to struggling with antimicrobial resistance, especially in case of multidrug-resistant microorganisms (Okkeh et al. 2021; Bruna et al. 2021; Gherasim et al. 2020; Zhang et al. 2015), which has become a serious threat over the last decades (Abushaheen et al. 2020; Frieri et al. 2017). Given the major mechanisms of antimicrobial activity for NPs, including reactive oxygen species (ROS) generation with subsequent damage to macromolecules such as DNA, phospholipids and proteins, cell membrane disruption, release of heavy metals binding to functional groups of proteins and inactivating them, inhibition of biofilm formation and bacterial efflux pumps, it is a more complicated task for microorganisms to develop resistance mechanisms compared with the conventional antibiotics (Lee et al. 2019; Niño-Martínez et al. 2019). However, molecular mechanisms through which metal NPs exert their antibacterial action are less specific against prokaryotes than eukaryotes in comparison with the traditionally used antibiotic agents. This suggests that the investigation of potential NPs-based antimicrobial agents requires a detailed analysis of their toxicity against the host cells. Furthermore, another strategy that is widely implemented to reduce the toxicity of metal NPs implies the application of polymer coating or incorporation of NPs into polymers (Floris et al. 2021; Długosz et al. 2020; Najahi-Missaoui et al. 2020). In addition to the safety profiles, biocompatible polymers improve pharmacokinetic effects and increase the therapeutic effectiveness of nanomaterials-based agents (Karabasz et al. 2020). In particular, noble metals can be embedded into polymers (Prakash et al. 2015). Gold (AuNPs) and silver nanoparticles (AgNPs) are widely used for diagnostic and therapeutic purposes, including as bioimaging, antibacterial and anticancer agents (Klębowski et al. 2018). Despite modifiable physicochemical properties and morphology, AuNPs and AgNPs are used in a limited way due to their non-selective action and toxicological effects. However, there is accumulating evidence that polymer matrices prevent the aggregation of metal NPs, increase their bioavailability and expand the range of biological activities (Reznickova et al. 2015). Particularly, nanosystems have been reported to be combined with antibodies, small biologically active molecules and photosensitizers to expand functional properties (Mohd-Zahid et al. 2021; Fadel et al. 2018; Feng et al. 2021; Elbaz et al. 2016). Furthermore, nanosystems have been demonstrated to acquire antioxidant properties after combination of AuNPs and AgNPs with plant extracts and some polymers (Zulfiqar et al. 2022; Maraveas et al. 2021). Antioxidant polymers of natural and synthetic origin have found their application in drug delivery, antimicrobial therapy, polymer biodegradation, etc. (Brito et al. 2021). Thus, the combination of a polymer component with AuNPs and AgNPs ensures the creation of general biologically active systems with a wide spectrum of activities and reduced cytotoxicity.

Experimental evidence suggests that dextran–co-polyacrylamide (D-PAA) polymer shows good biocompatibility (Tkachenko et al. 2022). This polymer can be used to develop D-PAA/AuNPs and D-PAA/AgNPs nanocomplexes as a platform for creating efficient multicomponent nanodrugs suitable for chemo- and photodynamic therapy (Chumachenko et al. 2016; Kutsevol et al. 2018; Kutsevol et al. 2022). İn the present study, we evaluated the antibacterial potential of D-PAA and its complexes with AuNPs and AgNPs providing some more insights into understanding the safety profile of these nanocomplexes. Thus, we focus on revealing their antibacterial effects supplementing our data with novel experimental findings on the toxicity of D-PAA polymer and AgNPs/AuNPs-D-PAA nanocomplexes against host cells.

Materials and methods

Reagents for synthesis of nanocomplexes

All chemicals used for the synthesis of nanocomplexes were purchased from *Merck* (Germany) and used without further purification except it was explicitly mentioned.

Polymer nanocarrier

Star-shaped D-PAA copolymer used as a matrix in the current study was synthesized using Ce^{4+}-initiated radical graft polymerization (Kutsevol et al. 2012). The average molecular weight of this polymer determined by size-exclusion chromatography was $Mw = 2.17 \times 10^6$ g/mol, while its polydispersity index was Mw/Mn = 1.56.

Synthesis of AuNPs/D-PAA nanocomplex

Initially, 0.5 mL gold precursor solution of $HAuCl_4$ (3×10^{-4} mol) was added to 5 mL D-PAA aqueous solution (1 g/L) and stirred for 20 min. Thereafter, the freshly prepared $NaBH_4$ solution (1.2×10^{-3} mol) was added dropwise during 1 min under vigorous stirring (Yeshchenko et al. 2018).

Synthesis of AgNPs/D-PAA nanocomplex

Firstly, 0.1 mL silver precursor solution of $AgNO_3$ (3×10^{-4} mol) was added to 5 mL D-PAA aqueous solution (1 g/L) and stirred for 20 min. Then freshly prepared $NaBH_4$ solution (1.2×10^{-3} mol) was added dropwise during 1 min under vigorous stirring (Chumachenko et al. 2014; Bulavin et al. 2016).

Dynamic light scattering

Dynamic Light Scattering (DLS) was performed on Malvern Zeta sizer (Malvern) provided with a 633 nm He–Ne laser. At least 7 correlation functions were recorded for each sample at a scattering angle of 173°. Particle size distribution (PSD) was estimated using inverse Laplace transforms implemented by regularized singular value decomposition using an approach reported earlier (Chumachenko et al. 2017).

Transmission electron microscopy (TEM)

The images of nanomaterials were obtained employing JEM 1000 (JOEL, Japan). Copper grids with a plain carbon film were used for sample preparation (Elmo, Cordouan Technologies, Bordeaux, France). A 5 µL drop was deposited and let adsorbed for 1 min, and then, the excess of the solution was removed with a piece of filter paper. Image processing and size measurements were conducted using *ImageJ 1.4* software.

Cultured fibroblasts

The primary fibroblast culture was obtained using the cells isolated from skin of rat embryos enzymatically (Sorokin et al. 2022). Cultivation was performed in Dulbecco's modified Eagle's medium (DMEM, Biowest, France) containing 10% fetal bovine serum (BioWhittaker® reagents, Lonza, Belgium) at 5% CO_2 and 37 °C up to passages 3–4. Culture medium was changed after 72 h of incubation.

Scratch assay

To perform the scratch assay, the fibroblasts were harvested by trypsinization and sub-cultured on 24-well plates (n = 6). As soon as the confluent monolayer was reached, the cells were scratched using a plastic pipette tip. D-PAA, AgNPs/D-PAA, and AuNPs/D-PAA nanocomplexes were added at concentrations of 0–2–5–10–20–30–50 mg/L. The width of cell-free area was determined following 24 h in 5 regions per well (Sorokin et al. 2022).

Proliferation assay

The fibroblasts were placed in 12-well plates at 10^5 cells per well for 24 h (n = 6). They were exposed to D-PAA, AgNPs/D-PAA, and AuNPs/D-PAA at 0–2–5–10–20–30–50 mg/L following the formation of monolayer. Following 72 h, the fibroblasts were harvested by trypsinization, and their doubling time was counted (Sorokin et al. 2022).

Micronucleus assay

After seeding the fibroblasts in 24-well plates (n = 6), they were treated with D-PAA, AgNPs/D-PAA, and AuNPs/D-PAA nanocomplexes at 0–2–5–10–20–30–50 mg/L. The cells were stained using Giemsa staining after 72 h. The number of fibroblasts with micronuclei was determined (Sorokin et al. 2022). Numerical data are expressed as % of cells containing micronuclei.

Antioxidant activity

Antioxidant activities of D-PAA, AgNPs/D-PAA and AuNPs/D-PAA were performed as reported earlier with some modifications (Salih Ağırtaş et al. 2015). UV–visible spectrophotometer was screened to evaluate the scavenging capacity of DPPH (2,2-diphenyl-1-picrylhydrazylradical). Due to its one-electron paramagnetic nature, DPPH behaves like a stable radical and color change is observed due to the reaction. The color change varies from purple to light yellow. The stock solutions of D-PAA, AgNPs/D-PAA and AuNPs/D-PAA were prepared at a concentration of 500 mg/L in DMSO. Thereafter, solutions with different concentrations (3.125–6.25–12.5–25–50 mg/L) were prepared from the stock solution by serial dilution. A total volume of 0.5 mL of each nanomaterial was transferred at different concentrations to test tubes used for the assay to be performed, and 2 mL of DPPH solution was added to each tube. After shaking vigorously, the test tubes were incubated for 30 min in the dark. Ascorbic acid (AA) and Trolox were used as references. When all steps of the assay were completed, the absorbance values of each solution were measured at 517 nm. The percentage of free radical scavenging activity of the tested samples expressed as the percent of DPPH inhibition (%), was calculated according to Formula 1.

$$\text{Capacity}\ (\%) = \left(\frac{\text{Abs (control)} - \text{Abs (sample)}}{\text{Abs (control)}}\right) \times 100 \quad (1)$$

DNA incision

Agarose gel electrophoresis (AGE) was used to examine the interactions of compounds with supercoiled pBR322 plasmid DNA. The complexes were incubated with pBR322 DNA for 120 min at 37.5 °C in the dark. Loading dye was added before D-PAA, AgNPs/D-PAA and AuNPs/D-PAA were loaded into a 1% agarose gel wells. Then AGE assay was performed in 1× TAE buffer at 110 V for 1 h. DNA images were acquired using a UV transilluminator.

Antimicrobial activity

Three gram-negative (−) bacteria, including *Escherichia coli* (ATCC 10,536), *Legionella pneumophila subsp. pneumophila* (ATCC 33,152), *Pseudomonas aeruginosa* (ATCC 9027), and three gram-positive (+) bacteria, such as *Staphylococcus aureus* (ATCC 6538), *Enterococcus hirae* and *E. faecalis* (ATCC 292,112), as well as two fungal species such as *Candida parapisilosis* and *Candida tropicalis* (ATCC 750), were used for the evaluation of the antimicrobial activity of D-PAA, AgNPs/D-PAA and AuNPs/D-PAA. All cultures were incubated at 37 °C overnight using nutrient broth (NB) as a medium. The antimicrobial activity of D-PAA, AgNPs/D-PAA and AuNPs/D-PAA was studied using 1:1 serial dilutions in 96-well microplates. After the dilution step, microbial inoculation was done and the samples were incubated for 24 h at 37 °C. The lowest D-PAA, AgNPs/D-PAA and AuNPs/D-PAA concentrations with no microbial growth were determined as the minimum inhibition concentration (MIC) value.

Antibiofilm activity

The studied nanomaterials were first added to the wells. Anti-biofilm activity was determined in a 24-well plate using different concentrations (62.5–125–250 mg/L) of D-PAA, AgNPs/D-PAA and AuNPs/D-PAA. Then cultured *S. aureus* and *P. aeruginosa* were added. Bacterial culture with no added nanostructured materials was used as a control. The prepared plates were further incubated at 37.5 °C for 3 days. When the incubation period was completed, the adherent cells remaining in the wells were gently washed twice with distilled water. The plates were then dried for 1 h at 80 °C. Upon completion, the plates were incubated for 1 h using crystal violet (CV) to stain the biofilms. CV was discarded and the plates were then slowly washed with distilled water

twice to remove remaining CV. Ethanol was added to extract CV measured using a spectrophotometer at 595 nm. The obtained values were processed according to Eq. (2).

$$\text{Biofilm inhibition}(\%) = \left(\frac{\text{Abs (control)} - \text{Abs (sample)}}{\text{Abs (control)}}\right) \times 100 \quad (2)$$

Cell viability

Microbial cell viability inhibition of D-PAA, AgNPs/D-PAA and AuNPs/D-PAA were investigated according to the method reported earlier (Gümüşgöz Çelik et al. 2022).

Statistical analysis

Data obtained in assays performed on cultured fibroblasts were statistically processed using GraphPad Prism 5.0 (USA) carrying out Kruskal–Wallis and Dunn's tests. P values below 0.05 were considered statistically significant. Data are shown as Me and IQR.

Results

Characterization of nanocomplexes

Analysis of TEM images (Fig. 1) confirms DLS radii values of 5.5 ± 2.0 nm and 5.0 ± 2.0 nm for Au and Ag NPs, respectively. Particle hydrodynamic radii (RH) distribution of D-PAA, AgNPs/D-PAA and AuNPs/D-PAA derived from DLS data are shown in Fig. 2. D-PAA PSD includes a single peak with a maximum at R_H = 40 nm corresponding to D-PAA macromolecules. As seen from PSD of AgNPs/D-PAA and AuNPs/D-PAA (Fig. 2, blue and red lines, respectively), the second intensive peak position didn't significantly change compared to D-PAA and corresponded to D-PAA macromolecules. The first peaks at maxima of R_H = 4 nm for AuNPs/D-PAA and R_H = 2.5 nm for AgNPs/D-PAA corresponded to AuNPs and AgNPs, respectively.

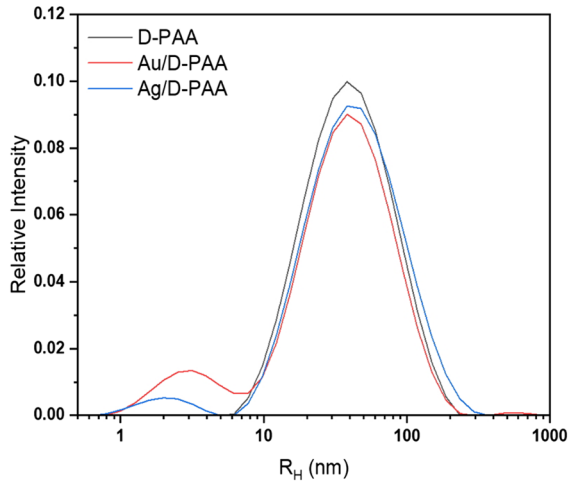

Fig. 2 Particle hydrodynamic radii distribution for D-PAA copolymer (black line), AuNPs/D-PAA (red line) and AgNPs/D-PAA

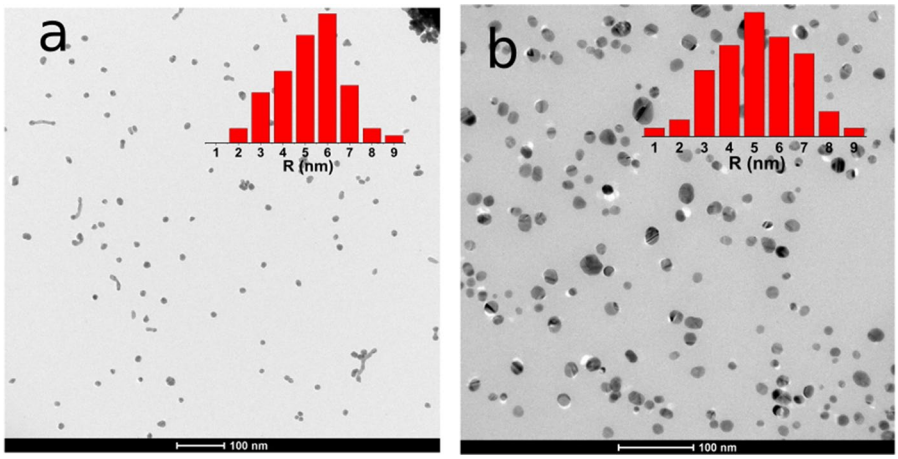

Fig. 1 TEM image and particle radii distribution of AuNPs/D-PAA (panel **a**) and AgNPs/D-PAA (panel **b**)

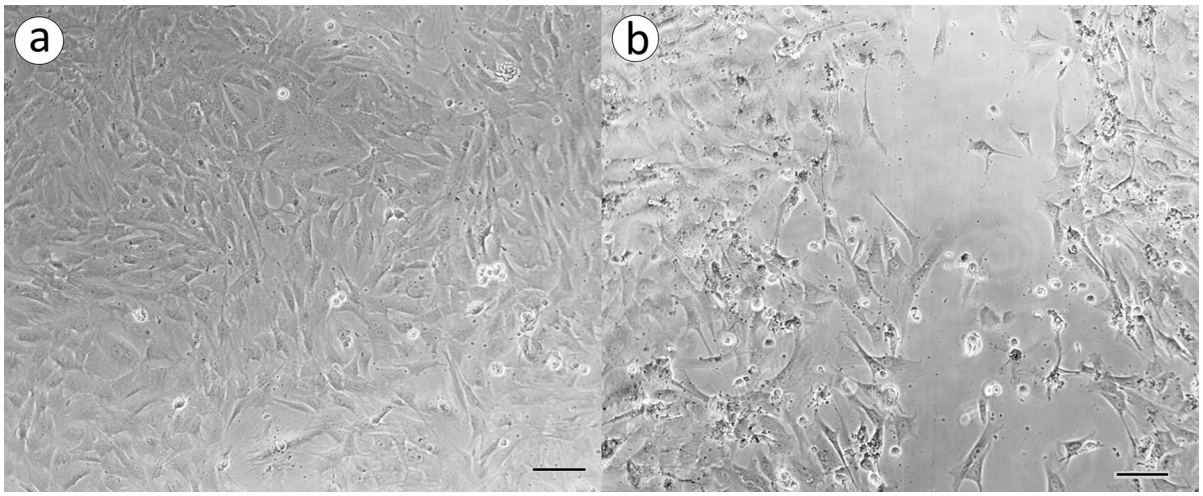

Fig. 3 Cultured fibroblast monolayer following scratching in a control sample (panel **a**) and following 24 h of exposure to AgNPs/D-PAA at 50 mg/L (panel **b**). Scale bar is 200 µm

Table 1 Quantitative analysis of migratory and proliferative capacities of fibroblasts exposed to DPAA, AgNPs/D-PAA and AuNPs/D-PAA nanocomposites

Parameter, unit		The width of scratch (scratch assay), µm	Doubling time (proliferation assay), h	Number of cells (proliferation assay), 10^6
Concentrations, samples				
0 mg/L	D-PAA AuNPs/D-PAA AgNPs/D-PAA	0.00 [0.00; 0.00]	146 [136; 150]	1.40 [1.30;1.53]
2 mg/L	D-PAA	0.00 [0.00; 0.00], $p > 0.05$	76 [70; 84], $p < 0.01$	1.95 [1.88; 2.08], $p < 0.01$
	AuNPs/D-PAA	0.00 [0.00; 0.00], $p > 0.05$	109 [105; 111], $p < 0.01$	2.00 [1.88; 2.13], $p < 0.01$
	AgNPs/D-PAA	0.00 [0.00; 0.00], $p > 0.05$	108 [103; 113], $p < 0.01$	1.60 [1.58; 1.65], $p > 0.05$
5 mg/L	D-PAA	176 [167; 186], $p > 0.05$	89 [83; 97], $p > 0.05$	1.85 [1.60; 1.90], $p > 0.05$
	AuNPs/ D-PAA	0.00 [0.00; 0.00], $p > 0.05$	103 [100; 115], $p < 0.01$	2.00 [1.93; 2.13], $p < 0.01$
	AgNPs/D-PAA	359 [321; 379], $p > 0.05$	105 [101; 111], $p < 0.01$	1.60 [1.50; 1.73], $p > 0.05$
10 mg/L	D-PAA	352 [328; 363], $p < 0.01$	90 [85; 96], $p > 0.05$	1.75 [1.53; 1.90], $p > 0.05$
	AuNPs/D-PAA	0.00 [0.00; 38.25], $p > 0.05$	145 [142; 150], $p > 0.05$	1.55 [1.48; 1.63], $p > 0.05$
	AgNPs/D-PAA	542 [499; 572], $p > 0.05$	148 [143; 151], $p > 0.05$	1.35 [1.25; 1.43], $p > 0.05$
20 mg/L	D-PAA	350 [331; 372], $p < 0.01$	119 [112; 124], $p > 0.05$	1.50 [1.18; 1.68], $p > 0.05$
	AuNPs/D-PAA	155 [129; 197], $p > 0.05$	0.00 [0.00; 0.00], $p < 0.001$	1.55 [1.48; 1.63], $p > 0.05$
	AgNPs/D-PAA	710 [673; 731], $p < 0.001$	0.00 [0.00; 0.00], $p < 0.001$	0.95 [0.80; 1.03], $p > 0.05$
30 mg/L	D-PAA	352 [342; 363], $p < 0.001$	151 [146; 163], $p > 0.05$	1.40 [1.38; 1.50], $p > 0.05$
	AuNPs/D-PAA	178 [103; 206], $p < 0.01$	Negative values	1.55 [1.38; 1.70], $p > 0.05$
	AgNPs/D-PAA	731 [674; 772], $p < 0.001$	Negative values	0.70 [0.60; 0.80], $p > 0.05$
50 mg/L	D-PAA	354 [317; 400], $p < 0.001$	230 [218; 238], $p > 0.05$	1.20 [1.08; 1.22], $p > 0.05$
	AuNPs/D-PAA	219 [210; 237], $p < 0.001$	Negative values	1.50 [1.38; 1.53], $p > 0.05$
	AgNPs/D-PAA	752 [705; 784], $p < 0.0001$	Negative values	0.55 [0.48; 0.63], $p < 0.001$

Scratch assay

As shown in Fig. 3, following 24 h, the confluent monolayers with spindle-shaped fibroblasts were observed in control samples. Low concentrations of nanocomplexes had no impact on cell migratory capacities. However, an increase in concentrations resulted in the reduced migration. AgNPs/D-PAA nanocomposite was found to have the highest inhibiting activity (Table 1; Fig. 3).

Proliferation assay

Low concentrations of D-PAA, AgNPs/D-PAA and AuNPs/D-PAA were shown to have the stimulatory effect on proliferation. AuNPs/D-PAA nanocomplexes reduced proliferation with increasing concentrations. AgNPs/D-PAA nanomaterials diminished the cell viability, since at a concentration of 20 mg/L, the number of collected cells was equal to the amount of the seeded ones, while a further increase in the concentrations of nanocomplexes was associated with a lower number of collected cells compared with the seeded ones (Table 1).

Micronucleus assay

As illustrated in Fig. 4, micronucleus assay revealed that D-PAA, AgNPs/D-PAA and AuNPs/D-PAA composites were of no genotoxicity at concentrations of 0–2–5–10–20–30–50 mg/L.

Antioxidant activity

The antioxidant activity of D-PAA, Ag/D-PAA and AuNPs/D-PAA are shown in Fig. 5. The antioxidant activity of D-PAA, Ag/D-PAA and AuNPs/D-PAA was found to be exhibited in a concentration-dependent manner. The antioxidant ability of D-PAA was determined as 17.86%, 20.44%, 37.81%, 45.07% and 61.33% at 3.125, 6.25, 12.5 mg/L, 25 mg/L and 50 mg/L, respectively. The radical scavenging activity of Ag/D-PAA was higher than that of D-PAA and AuNPs/D-PAA at all the tested concentrations. The highest antioxidant activity was 72.54% and 64.66% for Ag/D-PAA and AuNPs/D-PAA at 50 mg/L, respectively.

DNA incision

Plasmid pBR322 DNA-based DNA cleavage assay was used in this study. If a single break occurs in this pBR322 plasmid DNA molecule (Form I), Form II is formed. However, if a double strand break is observed, Form III is detected. These three forms of DNA, namely Form I, Form II, and Form III, are detected in agarose gel. As illustrated in Fig. 6, AgNPs/D-PAA and AuNPs/D-PAA showed single strand DNA cleavage activity at a concentration of 25 mg/L. In addition, both nanocomposites completely cleaved plasmid DNA at 50 and 100 mg/L.

Antimicrobial activity

Our findings on the antimicrobial activity of nanocomplexes are depicted in Table 2. The MIC values of D-PAA, AgNPs/D-PAA and AuNPs/D-PAA ranged from 16 mg/mL to 1024 mg/mL, which indicated different susceptibility of test bacteria to D-PAA, AgNPs/D-PAA and AuNPs/D-PAA. The MIC values of D-PAA were found to be 256 mg/mL for *E. faecalis* and *E. hirae*, 512 mg/mL for *E. coli*, *L. pneumophila subsp. pneumophila*, *S. aureus* and *C. tropicalis*, as well as 1024 mg/mL for *P. aeruginosa* and *C. parapisilosis*. The MIC values of AuNPs/D-PAA were determined to be 32 mg/mL for *E. hirae*, 64 mg/mL for *S. aureus*, *E. faecalis* and *C. tropicalis*, 128 mg/mL for *E. coli*, *P. aeruginosa* and *C. parapisilosis*, as well as 256 mg/mL for *L. pneumophila subsp. pneumophila*. As for AgNPs/D-PAA, this parameter was expectedly lower and varied from 16 mg/mL for *E. hirae*, 32 mg/mL for *S. aureus*, *E. faecalis* and *C. parapisilosis*, 64 mg/mL for *C. tropicalis*, 128 mg/mL for *E. coli* and *P. aeruginosa*, to 256 mg/mL for *L. pneumophilasubsp. pneumophila*. As seen in Table 2, AuNPs/D-PAA are much more effective than D-PAA, while the antimicrobial activity of AgNPs/D-PAA is superior to that of AuNPs/D-PAA.

Antibiofilm activity

In this study, the biofilm formation inhibition activity of D-PAA, AgNPs/D-PAA and AuNPs/D-PAA was investigated. Gram-positive *S. aureus* and

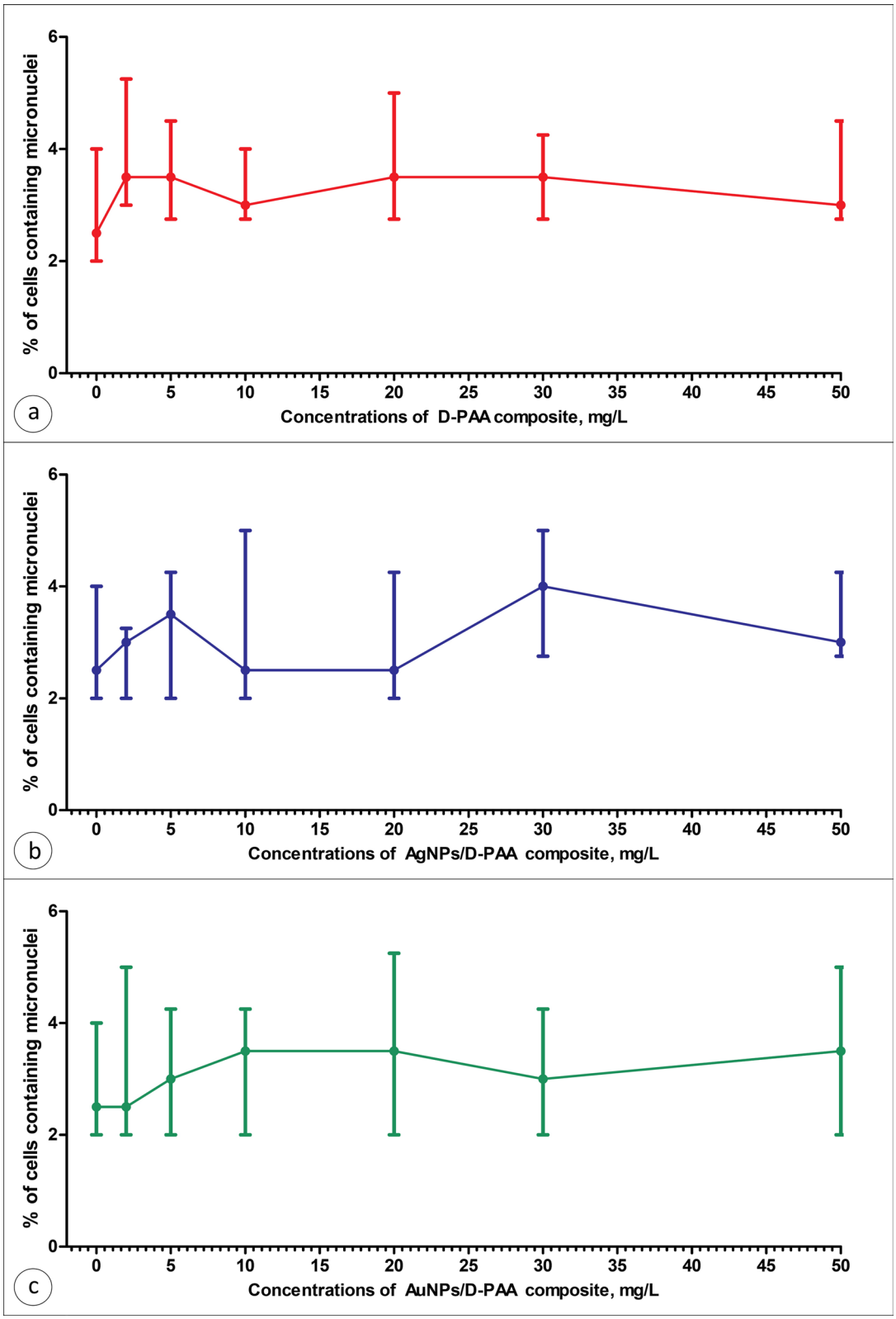
% of cells containing micronuclei
0
2
4
6
0 5 10 15 20 25 30 35 40 45 50
Concentrations of D-PAA composite, mg/L
a
% of cells containing micronuclei
0
2
4
6
0 5 10 15 20 25 30 35 40 45 50
Concentrations of AgNPs/D-PAA composite, mg/L
b
% of cells containing micronuclei
0
2
4
6
0 5 10 15 20 25 30 35 40 45 50
Concentrations of AuNPs/D-PAA composite, mg/L
c

◂**Fig. 4** Percentage of cells containing micronuclei following exposure to DPAA (panel **a**), AgNPs/D-PAA (panel **b**) and AuNPs/D-PAA (panel **c**) nanocomposites. No statistically significant differences are found ($p > 0.05$)

gram-negative *P. aeruginosa* strains were used to assess biofilm activity. The biofilm inhibition mediated by D-PAA, AgNPs/D-PAA and AuNPs/D-PAA are shown in Figs. 7 and 8. As the concentration of nanomaterials increased, anti-biofilm activity augmented in case of both microorganisms. When the concentration became higher from 62.5 mg/L to 125 mg/L, *S. aureus* biofilm inhibition activity increased from 74.98 to 90.13% for D-PAA, from 83.21 to 87.92% for AuNPs/D-PAA and from 86.49 to 92.33% for AgNPs/D-PAA. The highest anti-biofilm activity of D-PAA, AgNPs/D-PAA and AuNPs/D-PAA was detected to be 96.37%, 98.95% and 99.94% for *S. aureus* at 250 mg/L. The biofilm inhibition activity of D-PAA, AgNPs/D-PAA and AuNPs/D-PAA was found to be 38.97%, 75.12%, and 81.24% at 62.5 mg/L for *P. aeruginosa*, respectively, while biofilm inhibition activity at 125 mg/L was 61.13%, 80.67%, and 92.38%, respectively. Notably, the maximum biofilm inhibition activity of *P. aeruginosa* was determined at the level of 97.45% and achieved using AgNPs/D-PAA at 250 mg/L.

Microbial cell viability

In our study, the effects of newly synthesized D-PAA, AgNPs/D-PAA and AuNPs/D-PAA on cell viability of *E. coli* were investigated. The results are presented in Fig. 9.

The microbial cell viability inhibition was found to be 82.14%, 86.35% and 90.32% for D-PAA at 62.5 mg/L, 125 mg/L and 250 mg/L, respectively. The microbial cell viability inhibition caused by AgNPs/D-PAA was 100% at concentrations of 125 and 250 mg/L, while cell viability inhibition mediated by AuNPs/D-PAA was found to be 100% at a concentration of 250 mg/L.

Discussion

Nowadays one of the biggest issues in medicine is infections caused by resistant bacteria. This problem remains one of the most significant issues for the global health system and if no action is taken, it will cause bigger problems in the near future. For this reason, it is promising to carry out studies that aim at searching novel alternative products with antibacterial activity that cause the development of resistance in bacteria to a lesser extent than conventional antimicrobials (Karami et al. 2020). At the same time, they should show good host safety profiles. Collectively, fibroblast assays performed in this study demonstrate that AgNPs/D-PAA nanocomplexes have the highest toxicity. These data are consistent with previously reported features of the D-PAA, AgNPs/D-PAA and AuNPs/D-PAA toxicity profiles (Tkachenko et al. 2022) suggesting that they can be used for biomedical purposes at the concentrations below the toxicity threshold. Of note, our findings indicate that D-PAA shows low toxicity against prokaryotic cells, which is consistent with its toxicity profile in case of host cells (Tkachenko et al. 2022), while AgNPs/D-PAA nanocomplexes demonstrate the highest antimicrobial activity suggesting that they are more effective antibacterial agents compared to AuNPs/D-PAA. Furthermore, it is worth noting that AgNPs/D-PAA and AuNPs/D-PAA are more effective against gram-positive bacteria than gram-negative microorganisms. The observed antimicrobial effects of noble metal-based nanocomplexes may be at least partly attributed to oxidative stress, since they are capable of forming ROS and free radicals (Rai et al. 2012). It can be assumed that this mechanism along with metal ion release might contribute to the reduction of microbial viability observed in our study. However, the observed difference in effects between prokaryotic and host cells suggests that AgNPs/D-PAA and AuNPs/D-PAA may target some specific prokaryotic pathways. Studies that focus on uncovering specific bacterial signaling pathways targeted by NPs are strongly encouraged. Moreover, our data suggest that the antimicrobial activity of nanocomplexes differs between bacterial species indicating the presence of yet-to-be-discovered species-specific mechanisms.

Antibacterial activity of noble-metal nanocomplexes can be attributed to their antibiofilm properties as well. Biofilm formation ensures the protection of bacterial cells and their survival in hostile environments (Fulaz et al. 2019). Biofilm-forming microorganisms are known to be more resistant to the host immune system and less sensitive to antibiotics (Mahamuni-Badiger et al. 2020).

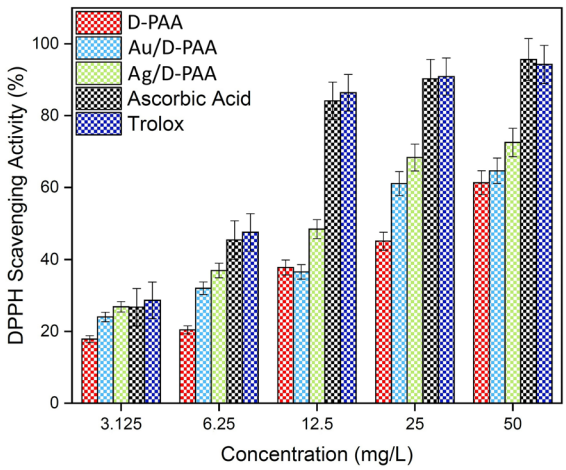

Fig. 5 2,2-Diphenyl-1-picrylhydrazyl radical scavenging activity (DPPH-test) after adding D-PAA, AuNPs/D-PAA and AgNPs/D-PAA

Expectedly, our data corroborate other experimental findings indicating the potential of noble metal-based nanomaterials as antimicrobial agents. Both pure noble metal NPs and their complexes (particularly with chitosan) demonstrate antibacterial activity with the effects more pronounced for Ag than Au (Alkhulaifi et al. 2020; Madakka et al. 2021; Mu et al. 2021). Of note, cellulose-based polymers influence antibacterial and antioxidant properties of AgNPs (Abdellatif et al. 2021), which is consistent with our data.

Abundant experimental evidence suggests that both AgNPs and AuNPs inhibit biofilm growth (Singh et al. 2018; Bharathi et al. 2018; Olfati et al. 2021; Goswami et al. 2015). Our findings indicate that the biofilm inhibitory activity of tested compounds, especially AgNPs/D-PAA and AuNPs/D-PAA, seems to be stronger compared to the effects of pure noble metal-based NPs observed in other studies, which can be related to the features of polymer. Antibiofilm activity of AgNPs/D-PAA and AuNPs/D-PAA demonstrated in this study reinforces the conclusions that there nanocomplexes are promising antibacterial agents, especially in case of resistant strains, due to their direct bactericidal effects and biofilm inhibition.

In addition to the antibacterial effects, the synthesized nanocomplexes clearly demonstrate ROS-scavenging capacities. ROS in cells play a dual role and are mainly generated due to leakage of electrons from the mitochondrial respiratory chain (especially complex I) (Yin et al. 2021). On the one hand, formation of ROS can cause cytotoxic effects due to accumulation of damaged macromolecules in cells, which is common for aging and multiple diseases. On the other hand, compelling evidence indicates that the role of ROS cannot be reduced to detrimental cell-damaging effects. Nowadays it is generally accepted that ROS perform regulatory functions acting as signaling molecules involved in pathways determining cell fate and survival (Sinenko et al. 2021; Sies and Jones 2020). Thus, ROS regulation by ROS-scavenging agents is an important strategy in the treatment of multiple diseases. Antioxidant properties of noble metal NPs have been shown in many studies (Turunc et al. 2021; Ravichandran et al. 2016; Ansar et al. 2020; Keshari et al. 2020; Milanezi et al. 2019; Sekar et al. 2022). Our study fully supports conclusions drawn earlier

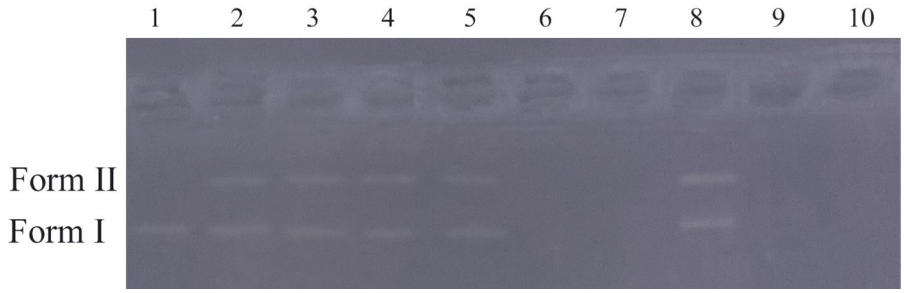

Fig. 6 DNA cleavage activity of D-PAA, AgNPs/D-PAA and AuNPs/D-PAA. Lane 1, pBR 322 DNA; Lane 2, pBR 322 DNA + 25 mg of D-PAA; Lane 3, pBR 322 DNA + 50 mg of D-PAA; Lane 4, pBR 322 DNA + 100 mg of D-PAA; Lane 5, pBR 322 DNA + 25 mg/L of AuNPs/D-PAA; Lane 6, pBR 322 DNA + 50 mg/L of AuNPs/D-PAA; Lane 7, pBR 322 DNA + 100 mg of AuNPs/D-PAA; Lane 8, pBR 322 DNA + 25 mg/L of AgNPs/D-PAA; Lane 9, pBR 322 DNA + 50 mg/L of AgNPs/D-PAA; Lane 10, pBR 322 DNA + 100 mg of AgNPs/D-PAA

Table 2 Antimicrobial activity of D PAA, AgNPs/D-PAA and AuNPs/D-PAA nanocomposites

Compounds	MIC values (mg/L)		
	D-PAA	AuNPs/D-PAA	AgNPs/D-PAA
E. coli	512	128	128
L. pneumophila subsp. pneumophila	512	256	256
P. aeruginosa	1024	128	128
S. aureus	512	64	32
E. hirae	256	32	16
E. faecalis	256	64	32
C. tropicalis	512	64	64
C. parapisilosis	1024	128	32

and indicate that the introduction of D-PAA polymer may reinforce or at least not reduce the antioxidant properties diminishing the overall toxicity.

Our study confirms earlier observations that AgNPs and AuNPs induce DNA cleavage (Gulbagca et al. 2019; Aygün et al. 2020; Zhao et al. 2008) providing some insights into the molecular mechanisms of NPs-induced cell damage. DNA damage inhibits the cell cycle and initiates apoptosis in eukaryotic cells. For bacteria, it can be accompanied by the loss of resistance-associated factors when a plasmid DNA is damaged or cell death when the chromosomal DNA is affected.

Thus, our findings show the versatility of biological effects of AgNPs/D-PAA and AuNPs/D-PAA

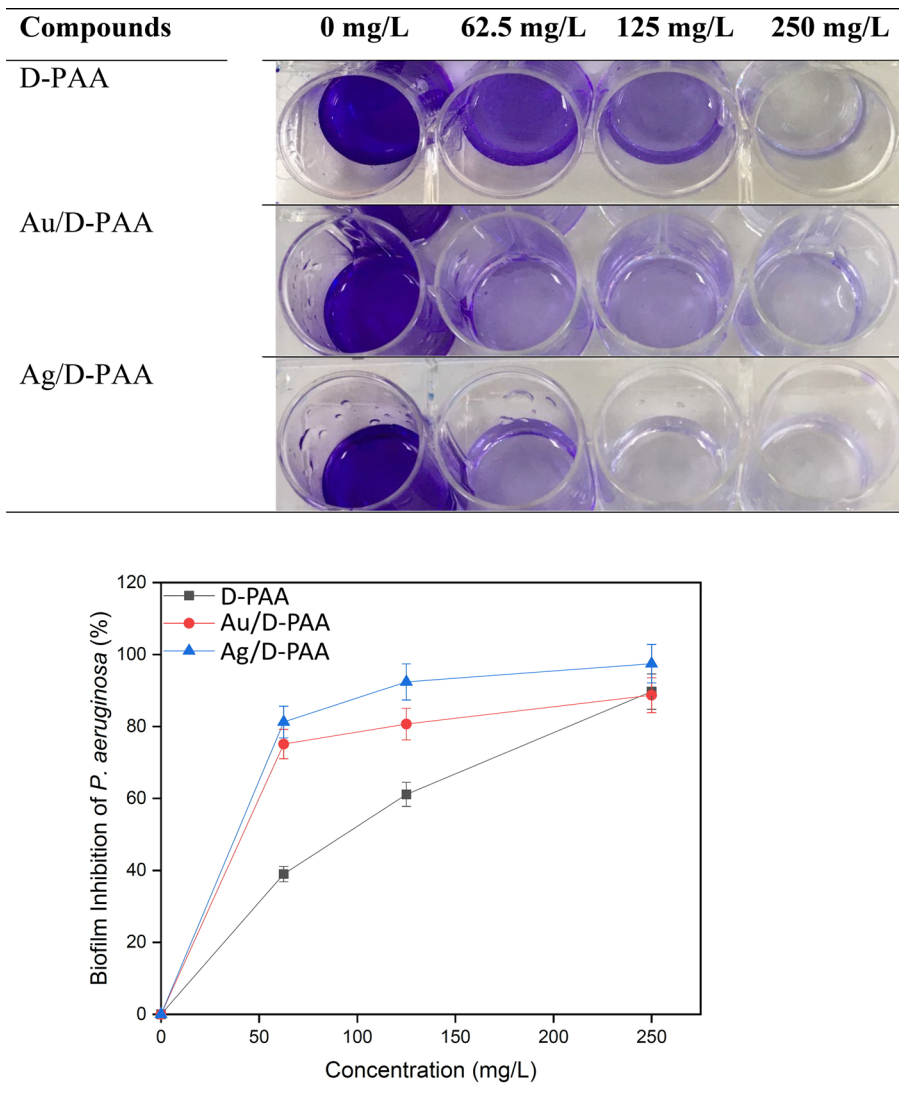

Fig. 7 AuNPs/D-PAA and AgNPs/D-PAA biofilm inhibition of *P. aeruginosa*

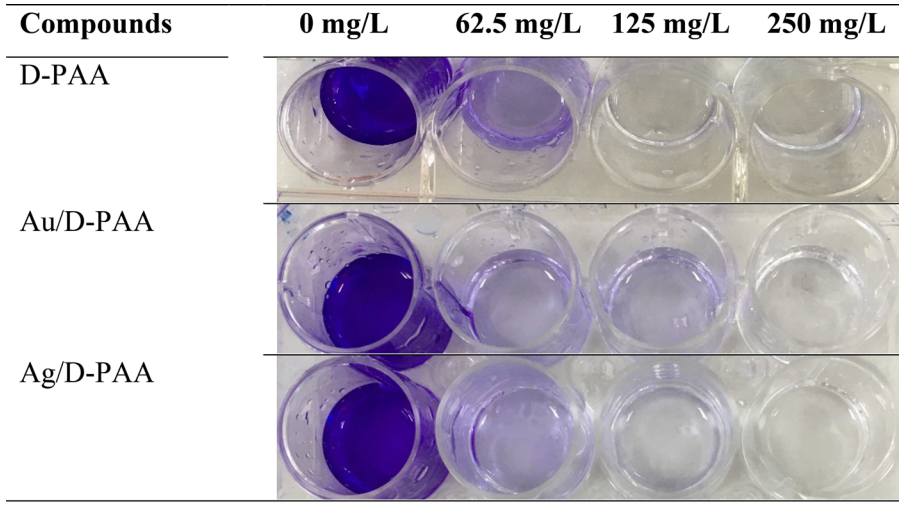

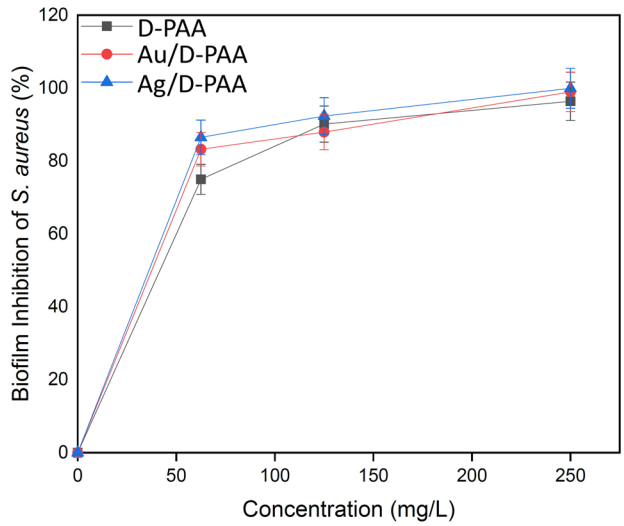

Fig. 8 AuNPs/D-PAA and AgNPs/D-PAA biofilm inhibition of *S. aureus*

ranging from antioxidant to antibacterial, biofilm-inhibiting effects and DNA cleavage. The presence of copolymer ensures modulation of noble metal NPs-mediated effects modifying the cytotoxicity. The current study aims at investigating the overall effects of nanocomplexes with no particular focus on the molecular mechanisms involved, which can be considered its limitation. To elucidate the underlying mechanisms, further research may focus on assessing the uptake of these nanocomplexes, metal ion release, ROS generation, and cell death pathways involved (apoptosis, necroptosis, autophagy-related cell death, ferroptosis, pyroptosis, cuproptosis, etc.). Moreover, identification of specific signaling pathways targeted by nanocomplexes in bacterial cells may shed light on the differences in toxic effects between eukaryotic and prokaryotic cells observed in the current study.

Conclusions

Our findings confirm that D-PAA is characterized by good tolerability and can be used to modify the properties of NPs as a component of nanocomposites. In general, D-PAA, nanocomplexes of AgNPs/D-PAA and AuNPs/D-PAA show good safety profile against primary cultured fibroblasts. However, AgNPs/D-PAA nanocomplex reduces migration of fibroblasts, while both AgNPs/D-PAA and AuNPs/D-PAA composites diminish cellular proliferation.

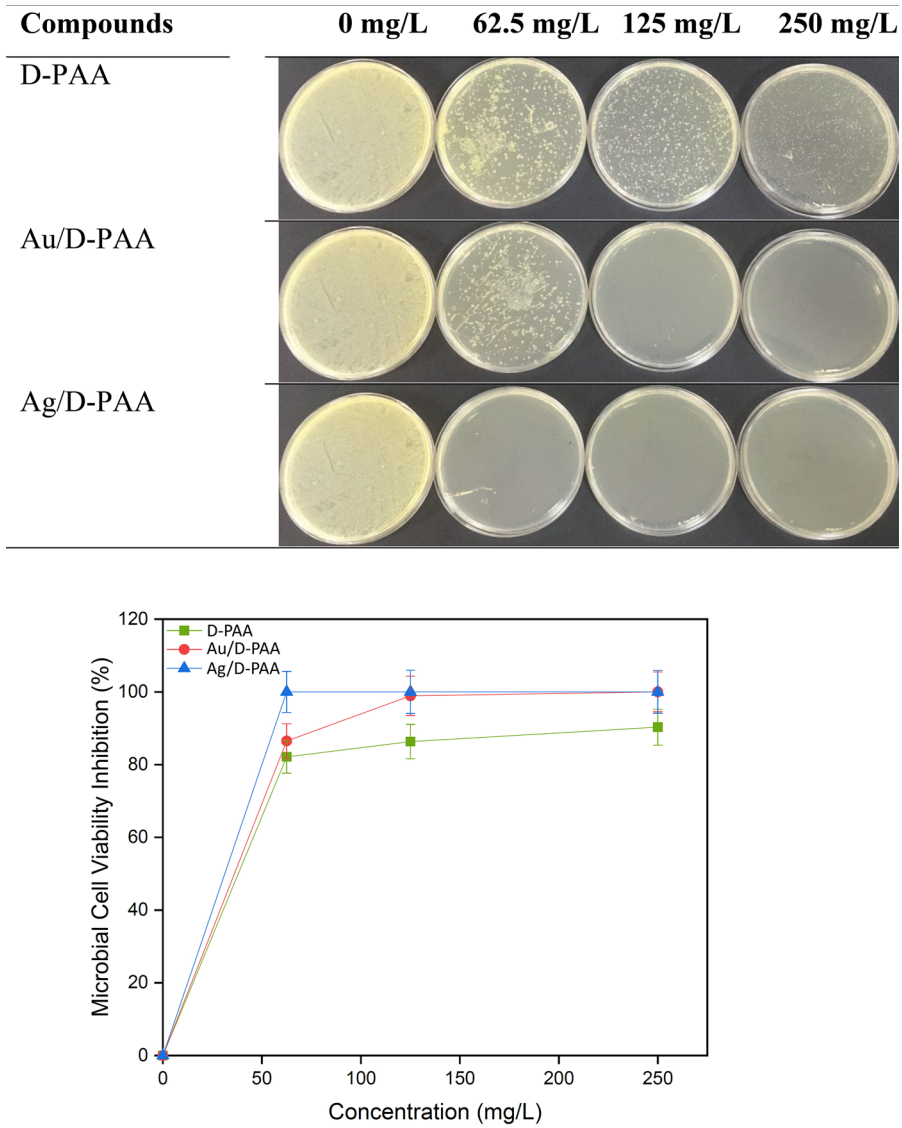

Fig. 9 *E. coli* growth inhibition of D-PAA, AuNPs/D-PAA and AgNPs/D-PAA

At the same time, all nanocomplexes show no genotoxicity. The studied nanocomplexes have antioxidant, antibacterial, biofilm-inhibiting and DNA cleavage-inducing activity. Antimicrobial effects of AgNPs/D-PAA are more pronounced against gram-positive bacteria, gram-negative bacteria, and fungi than those of D-PAA and AuNPs/D-PAA, especially against *E. hirae, E. faecalis* and *S. aureus*. D-PAA, AgNPs/D-PAA demonstrated the highest anti-biofilm activity. Nanosystems based on dextran–polyacrylamide polymers are promising agents for biomedical application.

Acknowledgements The authors thank to University of Strasbourg Institut Charles Sadron, French PAUSE program for emergency welcome of Ukrainian scientist Dr. Nataliya Kutsevol (2022–2023), Catherine Foussat and Mélanie Legros from the characterization group of the Institut Charles Sadron (Strasbourg, France) for size exclusion chromatography characterization of the star-shaped polymer.

Author contributions Conceptualization: AT, ND, NK; Original draft writing: AT, N.K; Experimental data acquisition: SÖ, GT, AO, VP, VC, PV, VP; Interpretation of data: SÖ, GT, KO, VP, AO; Statistical analysis: KO, AO; Funding: NK.

Funding This study was supported in part by the funds provided by the Ministry of the Education and Science of Ukraine, Project no. 0122U00181 (Hybrid nanosystems

based on "smart" polymers for biotechnology and medicine) and by National Research Foundation of Ukraine, Project 2020.02/0022 (Plasmon hybrid nanosystems "metal-polymer-fluorophore" with enhanced optical response for photonics and biomedical applications).

Data availability Data are available from the corresponding authors on reasonable request.

Declarations

Conflict of interest The authors declare no competing interests.

Ethical approval The study was approved by the Committee of Ethics and Bioethics at Kharkiv National Medical University, Kharkiv, Ukraine (minutes #3 dated 28 August 2020) and was performed in compliance with the EU Directive 2010/63/EU on the protection of animals used for scientific purposes.

References

Abdellatif AAH, Alturki HNH, Tawfeek HM (2021) Different cellulosic polymers for synthesizing silver nanoparticles with antioxidant and antibacterial activities. Sci Rep 11(1):84. https://doi.org/10.1038/s41598-020-79834-6

Abushaheen MA, Muzaheed, Fatani AJ, Alosaimi M, Mansy W, George M et al (2020) Antimicrobial resistance, mechanisms and its clinical significance. Disease-a-Month 66(6):100971. https://doi.org/10.1016/j.disamonth.2020.100971

Alkhulaifi MM, Alshehri JH, Alwehaibi MA, Awad MA, Al-Enazi NM, Aldosari NS et al (2020) Green synthesis of silver nanoparticles using citrus limon peels and evaluation of their antibacterial and cytotoxic properties. Saudi J Biol Sci 27(12):3434–3441. https://doi.org/10.1016/j.sjbs.2020.09.031

Ansar S, Tabassum H, Aladwan NSM, Naiman Ali M, Almaarik B, AlMahrouqi S et al (2020) Eco friendly silver nanoparticles synthesis by *Brassica oleracea* and its antibacterial, anticancer and antioxidant properties. Sci Rep 10(1):18564. https://doi.org/10.1038/s41598-020-74371-8

Aygün A, Özdemir S, Gülcan M, Cellat K, Şen F (2020) Synthesis and characterization of reishi mushroom-mediated green synthesis of silver nanoparticles for the biochemical applications. J Pharm Biomed Anal 178:112970. https://doi.org/10.1016/j.jpba.2019.112970

Bharathi D, Vasantharaj S, Bhuvaneshwari V (2018) Green synthesis of silver nanoparticles using *Cordia dichotoma* fruit extract and its enhanced antibacterial, antibiofilm and photo catalytic activity. Mater Res Express 5(5):055404. https://doi.org/10.1088/2053-1591/aac2ef

Brito J, Hlushko H, Abbott A, Aliakseyeu A, Hlushko R, Sukhishvili SA (2021) Integrating antioxidant functionality into polymer materials: fundamentals, strategies, and applications. ACS Appl Mater Interfaces 13(35):41372–41395. https://doi.org/10.1021/acsami.1c08061

Bruna T, Maldonado-Bravo F, Jara P, Caro N (2021) Silver nanoparticles and their antibacterial applications. Int J Mol Sci. https://doi.org/10.3390/ijms22137202

Bulavin L, Kutsevol N, Chumachenko V, Soloviov D, Kuklin A, Marynin A (2016) SAXS combined with UV–Vis spectroscopy and QELS: accurate characterization of silver sols synthesized in polymer matrices. Nanoscale Res Lett 11(1):35. https://doi.org/10.1186/s11671-016-1230-2

Chumachenko V, Kutsevol N, Rawiso M, Schmutz M, Blanck C (2014) In situ formation of silver nanoparticles in linear and branched polyelectrolyte matrices using various reducing agents. Nanoscale Res Lett 9(1):164. https://doi.org/10.1186/1556-276x-9-164

Chumachenko VA, Shton IO, Shishko ED, Kutsevol NV, Marinin AI, Gamaleia NF (2016) Branched copolymers dextran-graft-polyacrylamide as nanocarriers for delivery of gold nanoparticles and photosensitizers to tumor cells. In: Fesenko O, Yatsenko L (eds) Nanophysics, nanophotonics, surface studies, and applications. Springer, Cham

Chumachenko V, Kutsevol N, Harahuts Y, Rawiso M, Marinin A, Bulavin L (2017) Star-like dextran-graft-pnipam copolymers. Effect of internal molecular structure on the phase transition. J Mol Liq 235:77–82. https://doi.org/10.1016/j.molliq.2017.02.098

Długosz O, Szostak K, Staroń A, Pulit-Prociak J, Banach M (2020) Methods for reducing the toxicity of metal and metal oxide NPs as biomedicine. Materials (Basel). https://doi.org/10.3390/ma13020279

Elbaz NM, Ziko L, Siam R, Mamdouh W (2016) Core-shell silver/polymeric nanoparticles-based combinatorial therapy against breast cancer in-vitro. Sci Rep 6(1):30729. https://doi.org/10.1038/srep30729

Fadel M, Kassab K, Abd El Fadeel DA, Nasr M, El Ghoubary NM (2018) Comparative enhancement of curcumin cytotoxic photodynamic activity by nanoliposomes and gold nanoparticles with pharmacological appraisal in HepG2 cancer cells and Erlich solid tumor model. Drug Dev Ind Pharm 44(11):1809–1816. https://doi.org/10.1080/03639045.2018.1496451

Feng G-n, Huang X-t, Jiang X-l, Deng T-w, Li Q-x, Li J-x et al (2021) The antibacterial effects of supermolecular nano-carriers by combination of silver and photodynamic therapy. Front Chem. https://doi.org/10.3389/fchem.2021.666408

Floris P, Garbujo S, Rolla G, Giustra M, Salvioni L, Catelani T et al (2021) The role of polymeric coatings for a safe-by-design development of biomedical gold nanoparticles assessed in zebrafish embryo. Nanomaterials. https://doi.org/10.3390/nano11041004

Frieri M, Kumar K, Boutin A (2017) Antibiotic resistance. J Infect Public Health 10(4):369–378. https://doi.org/10.1016/j.jiph.2016.08.007

Fulaz S, Vitale S, Quinn L, Casey E (2019) Nanoparticle-biofilm interactions: the role of the EPS matrix. Trends Microbiol 27(11):915–926. https://doi.org/10.1016/j.tim.2019.07.004

Gherasim O, Puiu RA, Bîrcă AC, Burduşel AC, Grumezescu AM (2020) An updated review on silver nanoparticles in biomedicine. Nanomaterials (Basel). https://doi.org/10.3390/nano10112318

Goswami SR, Sahareen T, Singh M, Kumar S (2015) Role of biogenic silver nanoparticles in disruption of cell–cell adhesion in *Staphylococcus aureus* and *Escherichia coli* biofilm. J Ind Eng Chem 26:73–80. https://doi.org/10.1016/j.jiec.2014.11.017

Gulbagca F, Ozdemir S, Gulcan M, Sen F (2019) Synthesis and characterization of *Rosa canina*-mediated biogenic silver nanoparticles for anti-oxidant, antibacterial, antifungal, and DNA cleavage activities. Heliyon 5(12):e02980. https://doi.org/10.1016/j.heliyon.2019.e02980

Gümüşgöz Çelik G, Gonca S, Şahin B, Özdemir S, Atilla D, Gürek AG (2022) Novel axially symmetric and unsymmetric silicon(iv) phthalocyanines having anti-inflammatory groups: synthesis, characterization and their biological properties. Dalton Trans 51(19):7517–7529. https://doi.org/10.1039/D2DT00652A

Karabasz A, Bzowska M, Szczepanowicz K (2020) Biomedical applications of multifunctional polymeric nanocarriers: a review of current literature. Int J Nanomed 15:8673–8696. https://doi.org/10.2147/ijn.S231477

Karami A, Xie Z, Zhang J, Kabir MS, Munroe P, Kidd S et al (2020) Insights into the antimicrobial mechanism of Ag and I incorporated ZnO nanoparticle derivatives under visible light. Mater Sci Eng C 107:110220. https://doi.org/10.1016/j.msec.2019.110220

Keshari AK, Srivastava R, Singh P, Yadav VB, Nath G (2020) Antioxidant and antibacterial activity of silver nanoparticles synthesized by *Cestrum nocturnum*. J Ayurveda Integr Med 11(1):37–44. https://doi.org/10.1016/j.jaim.2017.11.003

Klębowski B, Depciuch J, Parlińska-Wojtan M, Baran J (2018) Applications of noble metal-based nanoparticles in medicine. Int J Mol Sci. https://doi.org/10.3390/ijms19124031

Kutsevol N, Bezugla T, Bezuglyi M, Rawiso M (2012) Branched dextran-graft-polyacrylamide copolymers as perspective materials for nanotechnology. Macromol Symposia 317(1):82–90. https://doi.org/10.1002/masy.201100087

Kutsevol N, Naumenko A, Chumachenko V, Yeshchenko O, Harahuts Y, Pavlenko V (2018) Aggregation processes in hybrid nanosystem polymer/nanosilver/cisplatin. Ukr J Phys 63(6):513. https://doi.org/10.15407/ujpe63.6.513

Kutsevol N, Kuziv Y, Bezugla T, Virych P, Marynin A, Borikun T et al (2022) Application of new multicomponent nanosystems for overcoming doxorubicin resistance in breast cancer therapy. Appl Nanosci 12(3):427–437. https://doi.org/10.1007/s13204-020-01653-y

Lee NY, Ko WC, Hsueh PR (2019) Nanoparticles in the treatment of infections caused by multidrug-resistant organisms. Front Pharmacol 10:1153. https://doi.org/10.3389/fphar.2019.01153

Madakka M, Jayaraju N, Rajesh N (2021) Evaluating the antimicrobial activity and antitumor screening of green synthesized silver nanoparticles compounds, using *Syzygium jambolanum*, towards MCF7 cell line (breast cancer cell line). J Photochem Photobiol 6:100028. https://doi.org/10.1016/j.jpap.2021.100028

Mahamuni-Badiger PP, Patil PM, Badiger MV, Patel PR, Thorat-Gadgil BS, Pandit A et al (2020) Biofilm formation to inhibition: role of zinc oxide-based nanoparticles. Mater Sci Eng C Mater Biol Appl 108:110319. https://doi.org/10.1016/j.msec.2019.110319

Maraveas C, Bayer IS, Bartzanas T (2021) Recent advances in antioxidant polymers: from sustainable and natural monomers to synthesis and applications. Polymers 13(15):2465

Milanezi FG, Meireles LM, de Christo Scherer MM, de Oliveira JP, da Silva AR, de Araujo ML et al (2019) Antioxidant, antimicrobial and cytotoxic activities of gold nanoparticles capped with quercetin. Saudi Pharm J 27(7):968–974. https://doi.org/10.1016/j.jsps.2019.07.005

Mohd-Zahid MH, Zulkifli SN, Che Abdullah CA, Lim J, Fakurazi S, Wong KK et al (2021) Gold nanoparticles conjugated with anti-CD133 monoclonal antibody and 5-fluorouracil chemotherapeutic agent as nanocarriers for cancer cell targeting. RSC Adv 11(26):16131–16141. https://doi.org/10.1039/D1RA01093J

Mu W, Fang W, Yao Y (2021) Synthesis of Ag@Au core-shell NPs loaded with ciprofloxacin as enhanced antimicrobial properties for the treatment and nursing care of *Escherichia coli* infection. Microb Pathog 150:104619. https://doi.org/10.1016/j.micpath.2020.104619

Najahi-Missaoui W, Arnold RD, Cummings BS (2020) Safe nanoparticles: are we there yet? Int J Mol Sci. https://doi.org/10.3390/ijms22010385

Niño-Martínez N, Salas Orozco MF, Martínez-Castañón GA, Torres Méndez F, Ruiz F (2019) Molecular mechanisms of bacterial resistance to metal and metal oxide nanoparticles. Int J Mol Sci. https://doi.org/10.3390/ijms20112808

Okkeh M, Bloise N, Restivo E, De Vita L, Pallavicini P, Visai L (2021) Gold nanoparticles: can they be the next magic bullet for multidrug-resistant bacteria? Nanomaterials (Basel). https://doi.org/10.3390/nano11020312

Olfati A, Kahrizi D, Balaky STJ, Sharifi R, Tahir MB, Darvishi E (2021) Green synthesis of nanoparticles using *Calendula officinalis* extract from silver sulfate and their antibacterial effects on *Pectobacterium caratovorum*. Inorg Chem Commun 125:108439. https://doi.org/10.1016/j.inoche.2020.108439

Prakash J, Pivin JC, Swart HC (2015) Noble metal nanoparticles embedding into polymeric materials: from fundamentals to applications. Adv Colloid Interface Sci 226:187–202. https://doi.org/10.1016/j.cis.2015.10.010

Rai MK, Deshmukh SD, Ingle AP, Gade AK (2012) Silver nanoparticles: the powerful nanoweapon against multidrug-resistant bacteria. J Appl Microbiol 112(5):841–852. https://doi.org/10.1111/j.1365-2672.2012.05253.x

Ravichandran V, Vasanthi S, Shalini S, Ali Shah SA, Harish R (2016) Green synthesis of silver nanoparticles using *Atrocarpus altilis* leaf extract and the study of their antimicrobial and antioxidant activity. Mater Lett 180:264–267. https://doi.org/10.1016/j.matlet.2016.05.172

Reznickova A, Novotna Z, Kvitek O, Kolska Z, Svorcik V, Gold (2015) Silver and carbon nanoparticles grafted on activated polymers for biomedical applications. J Nanosci Nanotechnol 15(12):10053–10073. https://doi.org/10.1166/jnn.2015.11689

Salih Ağırtaş M, Karataş C, Özdemir S (2015) Synthesis of some metallophthalocyanines with dimethyl 5-(phenoxy)-isophthalate substituents and evaluation of their antioxidant-antibacterial activities. Spectrochim Acta A Mol

Biomol Spectrosc 135:20–24. https://doi.org/10.1016/j.saa.2014.06.139

Sekar V, Al-Ansari MM, Narenkumar J, Al-Humaid L, Arunkumar P, Santhanam A (2022) Synthesis of gold nanoparticles (AuNPs) with improved anti-diabetic, antioxidant and anti-microbial activity from *Physalis minima*. J King Saud Univ Sci 34(6):102197. https://doi.org/10.1016/j.jksus.2022.102197

Sies H, Jones DP (2020) Reactive oxygen species (ROS) as pleiotropic physiological signalling agents. Nat Rev Mol Cell Biol 21(7):363–383. https://doi.org/10.1038/s41580-020-0230-3

Sinenko SA, Starkova TY, Kuzmin AA, Tomilin AN (2021) Physiological signaling functions of reactive oxygen species in stem cells: from flies to man. Front Cell Dev Biol. https://doi.org/10.3389/fcell.2021.714370

Singh P, Pandit S, Beshay M, Mokkapati V, Garnaes J, Olsson ME et al (2018) Anti-biofilm effects of gold and silver nanoparticles synthesized by the *Rhodiola rosea* rhizome extracts. Artif Cells Nanomed Biotechnol 46(sup3):S886-s99. https://doi.org/10.1080/21691401.2018.1518909

Sorokin A, Prokopiuk V, Grankina I, Borovoy I, Tkachenko A, Yefimova S (2022) Amphi-PIC J-aggregate-protein complexes: stability in blood and toxicity to cell cultures. *IEEE 12th International Conference Nanomaterials: Applications & Properties (NAP)*. https://doi.org/10.1109/NAP55339.2022.9934581

Tkachenko A, Virych P, Myasoyedov V, Prokopiuk V, Onishchenko A, Butov D et al (2022) Cytotoxicity of hybrid noble metal-polymer composites. Biomed Res Int 2022:1487024. https://doi.org/10.1155/2022/1487024

Turunc E, Kahraman O, Binzet R (2021) Green synthesis of silver nanoparticles using pollen extract: characterization, assessment of their electrochemical and antioxidant activities. Anal Biochem 621:114123. https://doi.org/10.1016/j.ab.2021.114123

Yeshchenko OA, Naumenko AP, Kutsevol NV, Maskova DO, Harahuts II, Chumachenko VA et al (2018) Anomalous inverse hysteresis of phase transition in thermosensitive dextran-graft-PNIPAM copolymer/Au nanoparticles hybrid nanosystem. J Phys Chem C 122(14):8003–8010. https://doi.org/10.1021/acs.jpcc.8b01111

Yin Z, Burger N, Kula-Alwar D, Aksentijević D, Bridges HR, Prag HA et al (2021) Structural basis for a complex I mutation that blocks pathological ROS production. Nat Commun 12(1):707. https://doi.org/10.1038/s41467-021-20942-w

Zhang Y, Shareena Dasari TP, Deng H, Yu H (2015) Antimicrobial activity of gold nanoparticles and ionic gold. J Environ Sci Health Part C 33(3):286–327. https://doi.org/10.1080/10590501.2015.1055161

Zhao W, Lam JCF, Chiuman W, Brook MA, Li Y (2008) Enzymatic cleavage of nucleic acids on gold nanoparticles: a generic platform for facile colorimetric biosensors. Small 4(6):810–816. https://doi.org/10.1002/smll.200700757

Zulfiqar H, Amjad MS, Mehmood A, Mustafa G, Binish Z, Khan S et al (2022) Antibacterial, antioxidant, and phytotoxic potential of phytosynthesized silver nanoparticles using *Elaeagnus umbellata* fruit extract. Molecules 27(18):5847